ISSN 0016-7932, Geomagnetism and Aeronomy, 2012, Vol. 52, No. 5, pp. 547–560. © Pleiades Publishing, Ltd., 2012.
Original Russian Text © L.I. Miroshnichenko, J.A. Pérez-Peraza, V.M. Velasco-Herrera, J. Zapotitla, E.V. Vashenyuk, 2012, published in Geomagnetizm i Aeronomiya, 2012, Vol. 52, No. 5, pp. 579–593.

Oscillations of Galactic Cosmic Rays and Solar Indices before the Arrival of Relativistic Solar Protons

L. I. Miroshnichenko[a, b], J. A. Pérez-Peraza[c], V. M. Velasco-Herrera[c], J. Zapotitla[c], and E. V. Vashenyuk[d]

[a] *Pushkov Institute of Terrestrial Magnetism, Ionosphere, and Radiowave Propagation, Russian Academy of Sciences, Troitsk, Moscow Region, 142190 Russia*

[b] *Skobeltsyn Research Institute of Nuclear Physics, Moscow State University, Moscow, 119991 Russia*

[c] *Instituto de Geofisica, Universidad Nacional Autónoma de México, CU, Coyoacán, 04510 México*

[d] *Polar Geophysical Institute, Apatity Division, Kola Scientific Center, Russian Academy of Sciences, Apatity, Murmansk Region, 184209 Russia*

e-mail: leonty@izmiran.ru

Received November 2, 2010; in final form, July 25, 2011

Abstract—Using modern wavelet analysis techniques, we have made an attempt to search for oscillations of intensity of galactic cosmic rays (GCR), sunspot numbers (SS) and magnitudes of coronal index (CI) implying that the time evolution of those oscillations may serve as a precursor of Ground Level Enhancements (GLEs) of solar cosmic rays (SCR). From total number of 70 GLEs registered in 1942–2006, the four large events – 23 February 1956, 14 July 2000, 28 October 2003, and 20 January 2005 – have been chosen for our study. By the results of our analysis, it was shown that a frequency of oscillations of GCR decreases as time approaches to the event day. We have also studied a behaviour of common periodicities of GCR and SCR within the time interval of individual GLE. The oscillations of GLE occurrence rate (OR) at different stages of the solar activity (SA) cycle is of special interest. We have found some common periodicities of SS and CI in the range of short (2.8, 5.2, 27 and 60 days), medium (0.3, 0.5, 0.7, 1.3, 1.8 and 3.2 years) and long (4.6 and 11.0 years) periods. Short and medium periodicities, in general, are rather concentrated around the maxima of solar cycles and display the complex phase relations. When comparing these results with the behaviour of OR oscillations we found that the period of 11 years is dominating (controlling); it is continuous over the entire time interval of 1942–2006, and during all this time it displays high synchronization and clear linear ratios between the phases of oscillations of η, SS and CI. It implies that SCR generation is not isolated stochastic phenomena characteristic exclusively for chromospheric and/or coronal structures. In fact, this process may have global features and involve large regions in the Sun's atmosphere.

DOI: 10.1134/S001679321205012X

1. INTRODUCTION

Solar proton events (SPEs) with large particle fluxes (SCRs) accelerated on the Sun are rather frequently observed near the Earth's orbit; they are one of the most important manifestations of solar activity (SA). These events have usually been considered as a random (stochastic) process mainly related to solar flares (see, e.g., (Miroshnichenko, 2001; Miroshnichenko and Pérez-Peraza, 2008)). At the same time, the close relationship of SPEs with SA centers, coronal mass ejections (CMEs), and shocks is also undoubted (Reames, 1999; Miroshnichenko, 2001). Finally, we can state that the occurrence rate of SPEs observed in the Earth's orbit generally follows the 11-year SA cycle (Miroshnichenko, 1992, 2001, 2003; Vashenyuk, 2000).

Most SPEs are observed in the nonrelativistic energy region (from ≥10 to ≤500 MeV for protons). SCR particles with such energies are mainly registered on spacecraft in the interplanetary space, in satellite orbits in the magnetosphere, and when balloons fly at stratospheric altitudes; in this case, such particles cause no effects at the Earth's surface. Oscillations in different SPE characteristics (specifically, the frequency and fluence of such events at proton energies of ≥10 and ≥30 MeV, etc.) were previously extensively studied (see, e.g., (Miroshnichenko, 1992, 2001, 2003)). Many periods typical of other SA parameters, specifically, periods of about 5 months and 2 years, were determined. Methods for predicting SCR fluxes with energies of ≥10 MeV for periods of up to 11 years were proposed with regard to these results (Miroshnichenko, 2003).

Relativistic solar protons with energies of 500 MeV to ≥10 GeV sporadically come to the Earth at an average occurrence rate of $\eta \sim 1.0$ a year. Such events were called ground level enhancements (GLEs). These events are usually registered at global neutron monitor (NM) and muon telescope (MT) networks on the Earth's surface. Seventy GLEs were registered from 1942 to 2006 (Miroshnichenko and Pérez-Peraza, 2008), and the first and last events were observed, respectively, on February 28, 1942 (GLE01), and December 13, 2006 (GLE70). The well-known extreme event of February 23, 1956 (GLE05), is still the greatest event during the entire history of observations. The second highest flux of relativistic protons among 70 GLEs was observed during the event of January 20, 2005 (GLE69), and we analyzed both extreme events (see below).

As is known, GLE events are mostly observed at the ascending or descending segments of the 11-year SS cycle curve (sometimes at the cycle maximum) and are almost absent during solar minimums (Nagashima et al., 1991; Vashenyuk, 2000; Miroshnichenko, 2001). Such a quasi-regularity in the η behavior was abruptly disturbed in cycle 22. For example, 13 GLEs were registered during three years (from July 1989 to June 1991) and only two additional SCR events during this cycle were registered in 1992. Thus, it is evident that only very strong fluctuations in the occurrence rate of individual GLEs can be observed against a background of quasiperiodic 11-year η variations (see, e.g., (Vashenyuk, 2000; Miroshnichenko, 2001, 2003; Miroshnichenko and Pérez-Peraza, 2008)).

Studying the SPE characteristics gives valuable information on the source properties, accelerated particle acceleration and transport processes, fundamental properties of the Sun as a star (e.g., the structure and dynamics of magnetic fields in the solar atmosphere), maximal potentialities of the solar accelerator (or accelerators), and the magnetic parameters of the interplanetary medium. On the other hand, it is still actual to provide radiation safety for spacecraft crews and electronics, especially when interplanetary missions are planned and performed (Miroshnichenko, 2003, 2005). Since the above fundamental and applied problems are of primary importance, we tried here to study the behavior of several cosmophysical and solar parameters before GLEs, for the first time using the up-to-date wavelet analysis technique (Torrence and Compo, 1998; Percival and Walden, 2000; Chui, 2001; Koronovskii and Khramov, 2003; Holmes and Lipo, 2003).

GCR oscillations are of primary importance among the studied parameters since they reflect the interplanetary medium state, namely, the turbulence level of the IMF where SCRs will propagate. The IMF turbulence level in turn depends on the SA level and character (sunspots, flares, CMEs, etc.). In this case, global disturbances of the circumsolar medium (up to the Earth's orbit) on large time scales depend on the SS number. The so-called coronal index (CI)—the corona brightness in the optical emission green region—is another important criterion of global SA. Thus, we are first of all interested in oscillations in three parameters that are directly or indirectly responsible for the most important (initial) conditions of SCR generation and transport. Further, we start to analyze the GLE occurrence rate (η) and, then, the relationship (coherence and synchronization) between this rate and oscillations in other parameters.

The preliminary results of our studies were briefly presented in (Pérez-Peraza et al., 2009, 2011a). The main methodical aim of our work is to demonstrate the possibilities and difficulties of the wavelet analysis method used to study SCRs and related solar and interplanetary phenomena. The elucidation of the fundamental regularities in the particle acceleration on the Sun and the search for observational criteria (precursors) for predicting GLEs are the promising physical and applied aspects of such a study. In Section 2 we described the research methods and characteristics of the applied observational data. Section 3 includes the results of a wavelet analysis oscillations of cosmic ray intensity. Of special interest are unique data on the variations of registration rate of GLEs (Section 4). At last, in Section 5 we critically discuss all obtained results and give our main conclusions.

2. ANALYSIS METHODS AND OBSERVATIONAL DATA

As was mentioned in (Christiansen et al., 2007), SA is often notable for nonlinear, short-term, and chaotic behaviour. Therefore, it seems reasonable to use the corresponding wavelet analysis methods in order to compare the observed variations in activity indicators with their mathematical models. Such a comparison will make it possible to better describe the behavior of the toroidal and poloidal magnetic fields of the solar dynamo. Wavelet analysis is a powerful tool for revealing the predominant oscillation mode and for studying the oscillation time evolution by transforming nonlinear time series into a "time–frequency" space (Torrence and Compo, 1998). On the other hand, wavelet analysis is a complicated and modernized version of harmonic analysis, when the latter is performed together with the compression of different data (e.g., solar and geophysical ones) in a wide region of applications (Kumar and Foufoula-Georgiou, 1997; Percival and Walden, 1993, 2000; Holmes and Lipo, 2003; Velasco et al., 2008). In particular, the wavelet analysis technique is often applied to time series in order to rapidly discover short-term phenomena. Note that an ordinary time series makes it possible to adequately localize a signal in time but does not include any information on the oscillation frequency. On the other hand, the Fourier transform gives a high frequency resolution but does not make it possible to localize a signal in time. In this connection, a wavelet is an "optimal" combination of the time localization and frequency characteristics of the studied oscillations.

Unfortunately, the primary data of GLE observations performed in 1942–1960 have several limitations since the number of cosmic ray stations was small and technical possibilities for registering SCRs were restricted at that time. Regular data obtained for several GLEs during that period were as a rule represented in the form of tables with average detector count rates for 15-min intervals. For certain events at individual stations, researchers managed to obtain 5- or even 1-min data (e.g., at the Ottawa and Chicago stations for the event of February 23, 1956); the data on the GCR intensity were averaged for an hour or day. On the other hand, the data on the solar indices (SS, the sum of SS areas, CI values, etc.) were represented as tables with average monthly, daily, or, at best, hourly values. Nevertheless, it is very interesting to process and analyze such archived data using new promising methods. For our analysis, we selected four extraordinary events (their serial numbers are given in parentheses): February 23, 1956 (GLE05); July 14, 2000 (GLE59); October 28, 2003 (GLE65); and January 20, 2005 (GLE69). The analyzed observational data were taken from the available NM databases (DataBase at World Data Center C, Japan; DataBase at World Data Center B, Russia).

The GCR intensity variations, i.e., the possible evolution of the GCR fluctuation power spectrum several days before a specific GLE instant, are of primary interest. To analyze the event of February 23, 1956, we used NM data at Mt. Climax (Canada); for the remaining three events, we analyzed the data from the Oulu station (Finland). In this case, we solved the diagnostic problem: to find singularities (oscillations) in the behavior of GCR and/or SCR fluxes before GLEs and/or within the GLE time intervals. This was performed in order to relate these oscillations to the known oscillations in other SA parameters (e.g., SS and CI also studied in the work) or to find new oscillations typical of SCR events. Finally, we studied the oscillations (fluctuations) in the GLE generation (observation) occurrence rate (η) during different solar cycle stages. For this purpose, we transformed the time series, including the registration dates of all 70 GLEs, into a "time–frequency" space (the so-called Pulse Width Modulation (PWM) series) (Holmes and Lipo, 2003), where the following denotations were accepted: *1*—there is a GLE event on a given day and *0*—there is no GLE event on a given day. However, we should note that the time scale for the majority of GLE events is given in minutes or tens of minutes, whereas the scale for the solar indices is usually much longer. Therefore, we used the daily scale for all time series in order to analyze the GLE coherence with other SA phenomena.

We compared the obtained data on the SCR event oscillation frequency, first of all, with the main SA characteristic, i.e., the behavior of the SS number (http://sidc.oma.be/sunspot-data/), which are widely used as an indicator of toroidal magnetic fields, solar dynamo, and activity as a whole. We also used a time series of the CI, i.e., a measure of the total solar radiation in the green coronal line with a length of 530.3 nm (Fe XIV). It is important to note that CI variations are comparable with oscillations in other similar indices for the full solar disk (the corresponding data are available on the website of the NOAA Data Center, Boulder, Co., United States: http://www.ngdc.noaa.gov/stp/SOLAR/solintro.html).

To detect the evolutionary changes in the spectrum of the main frequencies of the studied series, we applied the Morlet wavelet transform as a "mother" wavelet. The Morlet method is a useful instrument for analyzing localized variations in the fluctuation power density spectrum within the specified time series with a large set of frequencies. Such a procedure cannot be performed using classical Fourier analysis since we deal with nonstationary time series (Kumar and Foufoula-Georgiou, 1997). Coherent wavelet analysis is especially promising when time series and frequency intervals, where two phenomena strongly interact with each other, are studied in detail.

The significance level of the coherence of two time series on wavelet spectra (see below) is only determined using values within the so-called cone of influence (COI). As is known, errors will take place in the initial and final spectral regions (edge effects) as in usual spectral analysis, since statistical data are limited. The COI is the boundary of the spectral region where the edge effects become substantial. The COI parameter is determined as a time interval during which the spectrum power self-correlation decreases e times and the edge effects become negligible outside this interval. The U-shaped masks, corresponding to the COI boundaries in all figures in Sections 3 and 4, outline the regions with a confidence level of 95%.

We estimated the statistical significance level of the global wavelet spectrum (oscillation power density spectrum) using recent achievements in obtaining theoretical wavelet spectra for the white and red noise processes (Torrence and Compo, 1998). The figures given in Sections 3 and 4, illustrate the analyzed time series, present the wavelet spectra for oscillations in several parameters, and demonstrate the oscillation power density spectra. CR intensity time profiles are presented at the top of the right-hand side panels; the oscillation wavelet spectra are shown below; the left-hand side panels demonstrate the corresponding power density spectra. The lighter zones of the wavelet diagrams correspond to oscillations with high levels of power or coherence (*1*) between both spectra. Low-intensity oscillations or oscillations with a low coherence level (*0*) are colored deep black. The power spectrum significance level is marked by dotted lines in the figures; these lines correspond to the red noise spectrum power (Gilman et al., 1963) at a confidence level of 95%. Therefore, we recall that the red noise power increases with decreasing frequency, i.e., with increasing oscillation period (Grinsted et al., 2004).

The phase relationships between the power density spectra for the two studied time series are shown by arrows. The horizontal arrows directed to the right (0°) correspond to the coincidence of phases when the relationship between them is positive linear; the situations when the phases are opposite at a negative linear relationship between them are marked by leftward horizontal arrows (180°). The arrows that are at any other angle correspond to a more complex (nonlinear) relationship between two phenomena (Velasco and Mendoza, 2008). The model (analog) PWM time series makes it possible to reveal and study the *coherence* and *synchronization* between the GLE event frequency and the corresponding series of the SS and CI indices.

The results of a wavelet analysis of the oscillation spectrum for four studied GLEs are described below. More detailed results are given, for example, for the two extreme events GLE05 (February 23, 1956) and GLE69 (January 20, 2005). The GLE registration rate η (for the dates of events during the entire period from 1942 to 2006) is subsequently analyzed, and the results of studying the coherence and synchronization of the η data with the data on the SS and CI are finally presented. The conditional scale of the global wavelet spectrum power density is shown near each panel (on the right-hand side) in Figs. 1–9 presented below; the calculated power density of red noise at a confidence level of 95% is marked by a dotted line. As in (Mendoza et al., 2006; Velasco and Mendoza, 2008; Velasco et al., 2008), as a red noise model, we used the AR1 autoregression model of the first order (the Markovian process) with the characteristic parameter $\alpha = 0.72$, selected according to the recommendations given in (Torrence and Compo, 1998).

3. OSCILLATIONS OF COSMIC RAYS

Before we consider the main results, we note that we start our analysis with wavelet diagram calculations for GCR oscillations with an anticipation period from 14 days to the first day before a specific GLE. The GCR oscillations up to an SCR event are evidently of diagnostic value since they in turn reflect the state (the level of disturbance) of the interplanetary medium where relativistic protons will soon propagate from the Sun. It is natural to assume that the role of SCRs is decisive on the day of an event and their contribution to oscillations will increase with increasing GLE power (i.e., with increasing SCR flux enhancement amplitude). Therefore, it is unclear what is the contribution of oscillations caused by GCRs in GLE events of different power? In particular, when GLEs are small, we can anticipate that their contribution to general oscillations will be insignificant at least based on observations on the Earth's surface. The situation can be opposite if GLEs are very powerful.

On the other hand, the SCR intensity time profile and the GLE power depend on several factors, which are not directly related to the event formation on the Sun (e.g., on the heliolongitudinal distance between the locations of a flare and an observational point, geomagnetic cutoff rigidity, asymptotic cone of acceptance of coming radiation at a given station, etc.). Therefore, the wavelet diagram shape can depend on the selected events and on the position and number of the stations selected for studying a given event. At the same time, it seems probable that some similar characteristics, which can be of prognostic value for GLE prediction techniques, will manifest themselves in the GCR oscillation behavior at least before powerful GLEs. In this case, the high GCR and SCR registration accuracy at the global NM network makes it possible to study oscillations with periods of ≤1 day in contrast to the data on solar indices (e.g., the SS and CI), which are not measured more frequently than once a day, limiting the study of oscillations.

At the same time, our analysis indicated (see Section 4) that the SS and CI solar indices are useful for studying the relationship (coherence and synchronization) between the GLE occurrence rate (η) and SA level on large timescales in spite of the limitations mentioned above. The data obtained in this case can be of certain value for predicting at least large GLE events. Thus, in our study, using the wavelet analysis technique, we implement a complex approach to the search for different-period oscillations and use different data series (GCRs, SCRs, SS, and CI), which can be related to the preparation and implementation of an SCR event.

Event of February 23, 1956. Figures 1 and 2 show the evolution of the GCR oscillation spectrum before and during the GLE05 event registered after the flare that occurred on February 23, 1956 (its heliocoordinates are 23°N, 80°W; the power was 3B). An analysis was performed using 5-min data from the Climax station (the ordinate is given in terms of the neutron monitor count rate) for the three-month interval from January 1 to March 31, 1956 (91 days); the sampling time is 1 day. To construct specific wavelet diagrams, we selected three intervals: (1) January 1–February 9, i.e., 14 days before the event; (2) January 1–February 22, i.e., one day before the SCR arrival; and (3) the latter pair of plots (bottom, right) was constructed for the entire interval from January 1 to March 31, including the GLE day.

The top panels in Fig. 1 demonstrate CR intensity time profiles, including the SCR flux arrival from the flare that occurred on February 23, 1956; the bottom panels present wavelet diagrams of oscillations in the particle intensity. The abscissa reflects the actual time in days, beginning from January 1, 1956; the oscillation periods along the ordinate on the left-hand side are given in days. The corresponding spectra of the fluctuation power density in arbitrary units (the abscissa) are given from top to bottom on the left-hand side panels, depending on the period in days (the ordinate). The upper two pairs of plots can be used to trace the time evolution of oscillation periods in going from the interval January 1–February 9 to the interval January 1–February 22: a weak tendency towards energy

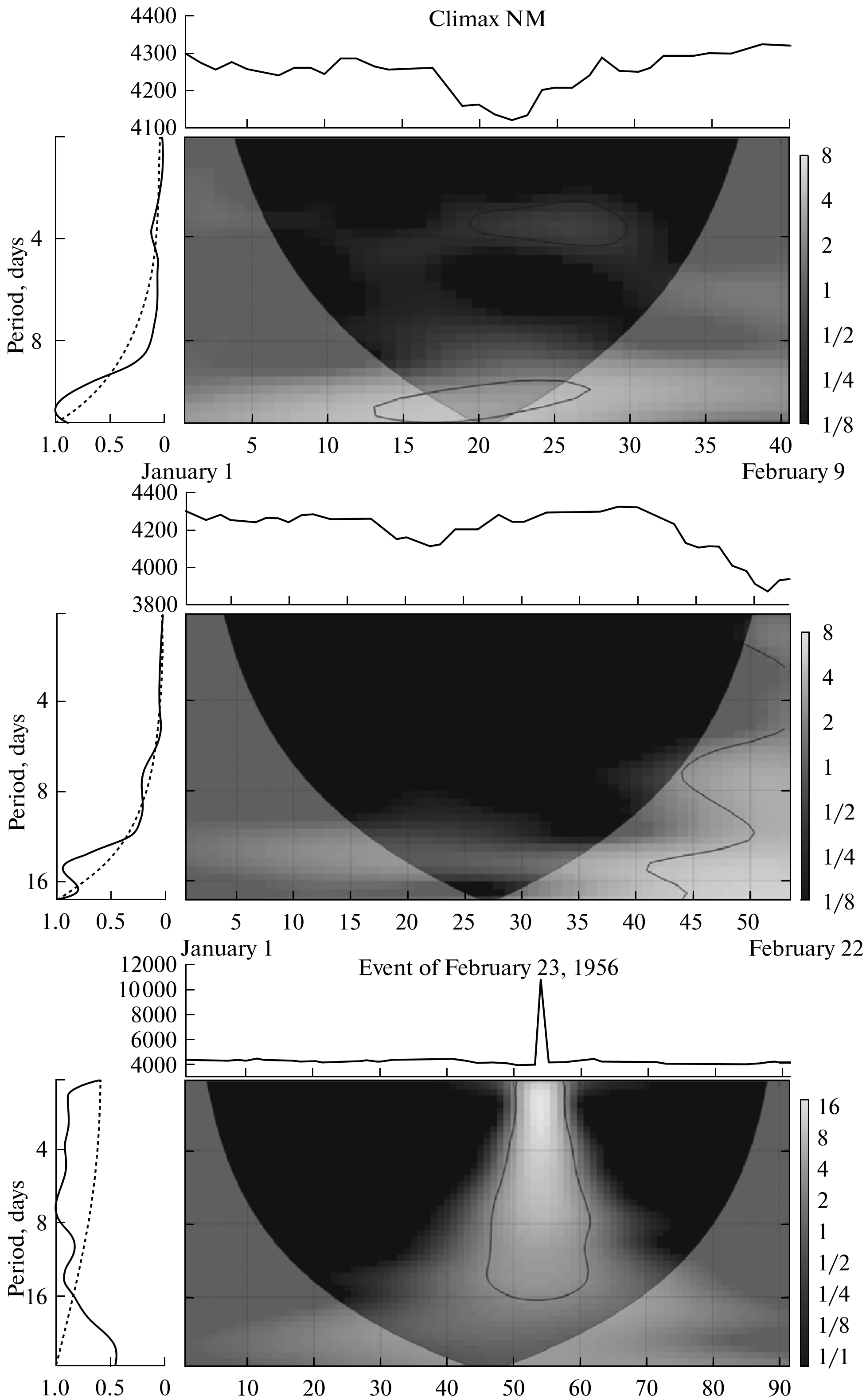

Fig. 1. Intensity time profiles and wavelet spectra of GCR oscillations 14 days before the event of February 23, 1956 (the right-hand side panel, the upper pair of plots), a day before the event (the middle pair), and during the entire studied interval from January 1 to March 31, 1956, including the GLE day (the bottom pair). The corresponding oscillation power spectra in arbitrary units (the abscissa axis) are given on the left-hand side panels depending on the period in days (the ordinate axis). Hereafter, the red noise power at a confidence level of 95% is marked by a dotted line and the spectrum power conditional scale is shown near each panel on the right-hand side.

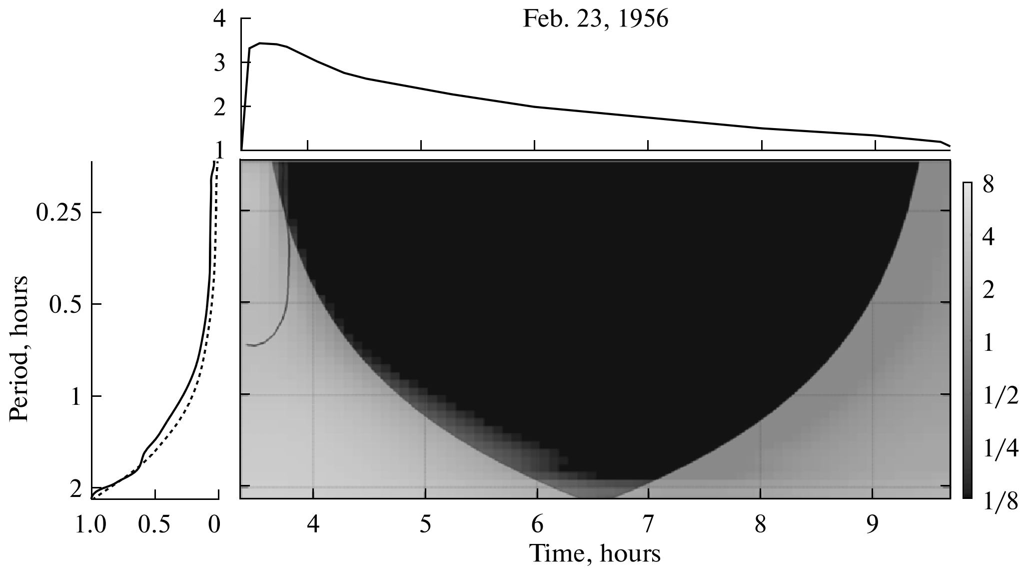

Fig. 2. SCR intensity time profile (top right-hand side) and CR oscillation wavelet spectrum on the event day of February 23, 1956 (bottom). The SCR flux along the ordinate is shown in arbitrary units, and the time is counted off in hours from the event onset; the oscillation periods (the ordinate axis) are expressed in hours. The oscillation power density spectrum in arbitrary units (the abscissa axis) is given on the left-hand side depending on the period (the ordinate axis, hours).

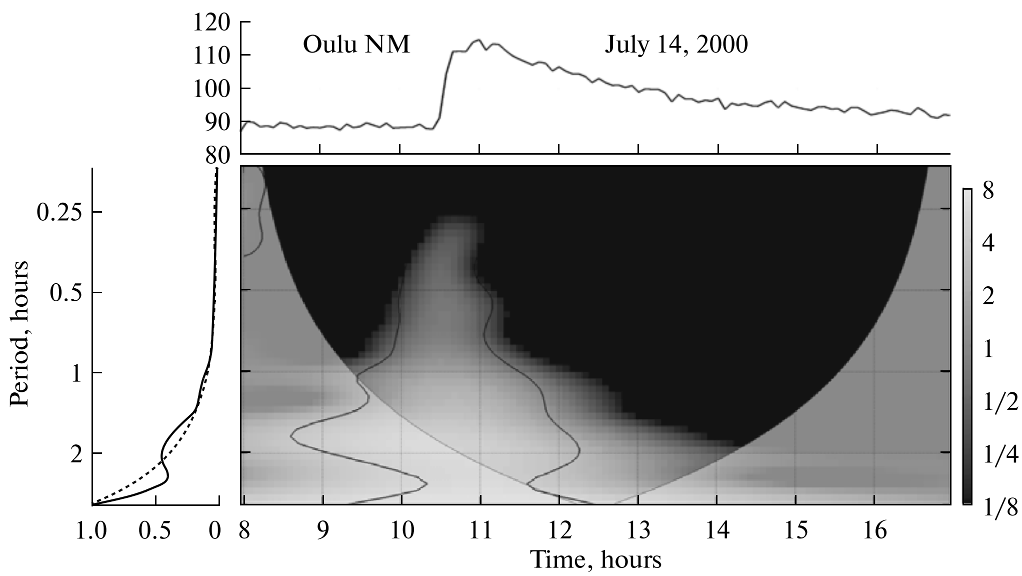

Fig. 3. Time profile (top) and wavelet diagram of the SCR flux oscillations observed on July 14, 2000 (bottom); the SCR flux at the Oulu station (the ordinate axis) is given in arbitrary units, and the time (the abscissa axis) is counted off in hours; the oscillation periods (the ordinate axis) are expressed in hours. The oscillation power density spectrum in arbitrary units (the abscissa axis) is given on the left-hand side depending on the period (the ordinate axis, hours).

pumping from short periods to longer ones is observed in the power spectrum; i.e., the oscillation frequency decreases. The power distribution between periods changes sharply if the entire studied interval is considered (from January 1 to March 31, 1956). The lower pair of plots in Fig. 1 makes it possible to observe that the power spectrum is complex (quasi-continuum) owing to the GLE contribution and oscillations with periods shorter than eight days predominate.

To detect the GLE/SCR effect, we present in Fig. 2 (right, top) the time profile of relativistic solar protons on the day when the event of February 23, 1956, occurred and the wavelet spectrum of the total GCR and SCR flux oscillations (bottom); the power density spectrum of the discovered oscillations is demonstrated on the left-hand side. These plots allow us to conclude that the characteristic CR fluctuation periods were distributed smoothly during the GLE05

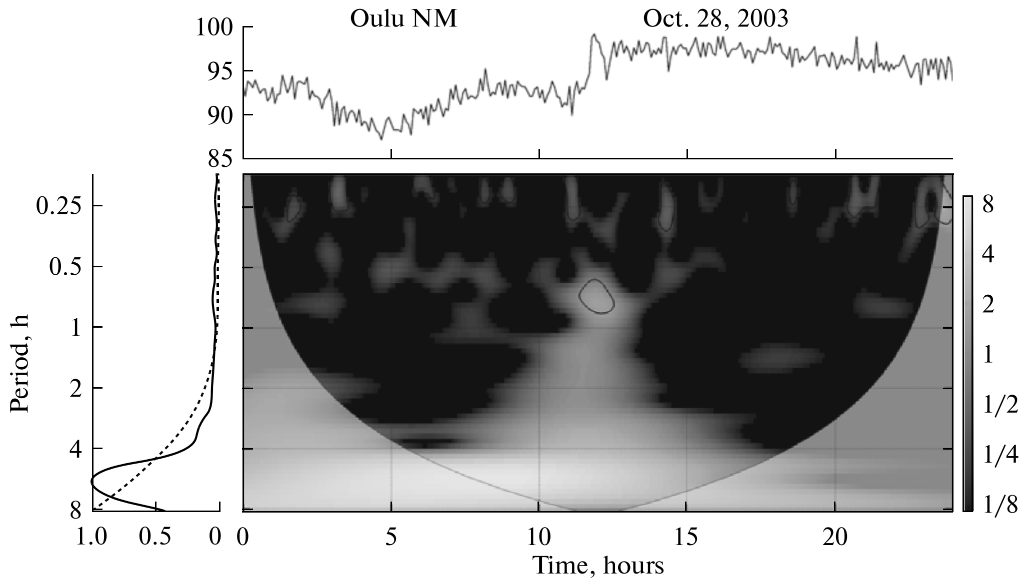

Fig. 4. Time profile (top) and wavelet diagram of SCR flux oscillations on October 28, 2003 (bottom); the SCR flux at the Oulu station (the ordinate axis) is shown in arbitrary units, and the time (the abscissa axis) is counted off in hours. The oscillation power density spectrum in arbitrary units (the abscissa axis) is given on the left-hand side depending on the period (the ordinate axis in hours).

event, beginning from ~15 min to ≥2 h. Such a range of periods most probably means that SCRs mostly contributed to CR oscillations during a GLE. However, the power density only insignificantly exceeds the calculated red noise level for all indicated periods.

Event of July 14, 2000. The GLE59 event was analyzed based on the Oulu NM data; the corresponding flare had heliocoordinates of 22°N, 07°W and a power of 3*B*/*X*5.7. This event is often called the Bastille Day Event (BDE). The time variations in the flux of relativistic solar protons on the event day are shown in Fig. 3 (right, top); a wavelet diagram of the proton flux oscillations is given at the bottom; and the left-hand side plot shows the oscillation power density spectrum. It is clear that the most significant level of SCR fluctuations above the red noise level was ~1.7 h on July 14, 2000.

Event of October 28, 2003. As in the previous case (GLE59), we analyzed GLE65 using the Oulu NM data. The corresponding flare had heliocoordinates of 20°S, 02°E and a power of 4*B*/*X*17. The results of a wavelet analysis are presented in Fig. 4 in the same terms as in Fig. 3. The power density spectrum (the left-hand side plot) indicates that oscillations with periods of ~15 to ~45 min (the level of these oscillations was slightly higher than that of red noise) and ~7 h (the latter peak was most significant) took place on October 28, 2003.

Event of January 20, 2005. Figure 5 presents the results of a detailed wavelet analysis of oscillations for the event that took place on January 20, 2005 (GLE69). The corresponding flare had heliocoordinates of 14°N, 61°W and a power of 2*B*/*X*7.1, which slightly resembles the close characteristics of the flare that occurred on February 23, 1956. We performed an analysis using the Oulu NM data with different time averaging beginning from 10 min. The analyzed interval was 31 days (entire January, 2005). We selected three intervals in order to construct specific wavelet spectra: (1) January 1–14, i.e., five days before the event; (2) January 1–19, i.e., a day before the SCR arrival; and (3) January 1–31, including the GLE day. The upper curves on the right-hand side panels correspond to the CR intensity time profiles, including an SCR intensity enhancement on January 20, 2005; the lower diagrams represent the wavelet spectra of particle intensity oscillations. The abscissa reflects the real time in days for January, and the periods are shown in days (the left-hand side ordinate axis). The corresponding power density spectra of fluctuations (oscillations) are shown from top to bottom on the left-hand side panels in arbitrary units (the abscissa axis), depending on the period in days (the ordinate axis). As in the GLE05 case, the oscillation periods on the lef-hand side in Fig. 5 show a tendency towards an increase as the event day approaches. At the same time, in contrast to the event of February 23, 1956 (Fig. 1, on the left-hand side), the power density spectra of GCR oscillations from 5 days to 1 day before the GLE69 event are much lower than the red noise level. If the entire studied interval is considered (January 1–31, 2005), it is clear that the power spectrum has a predominant peak near the ~3.5-h period (the lower pair of the plots) owing to the GLE/SCR contribution.

Figure 6 (the left-hand side panel) shows the SCR intensity profile (top) and the wavelet spectrum of their oscillations (bottom) on the GLE69 event day on a larger scale. The intensity plot and the wavelet dia-

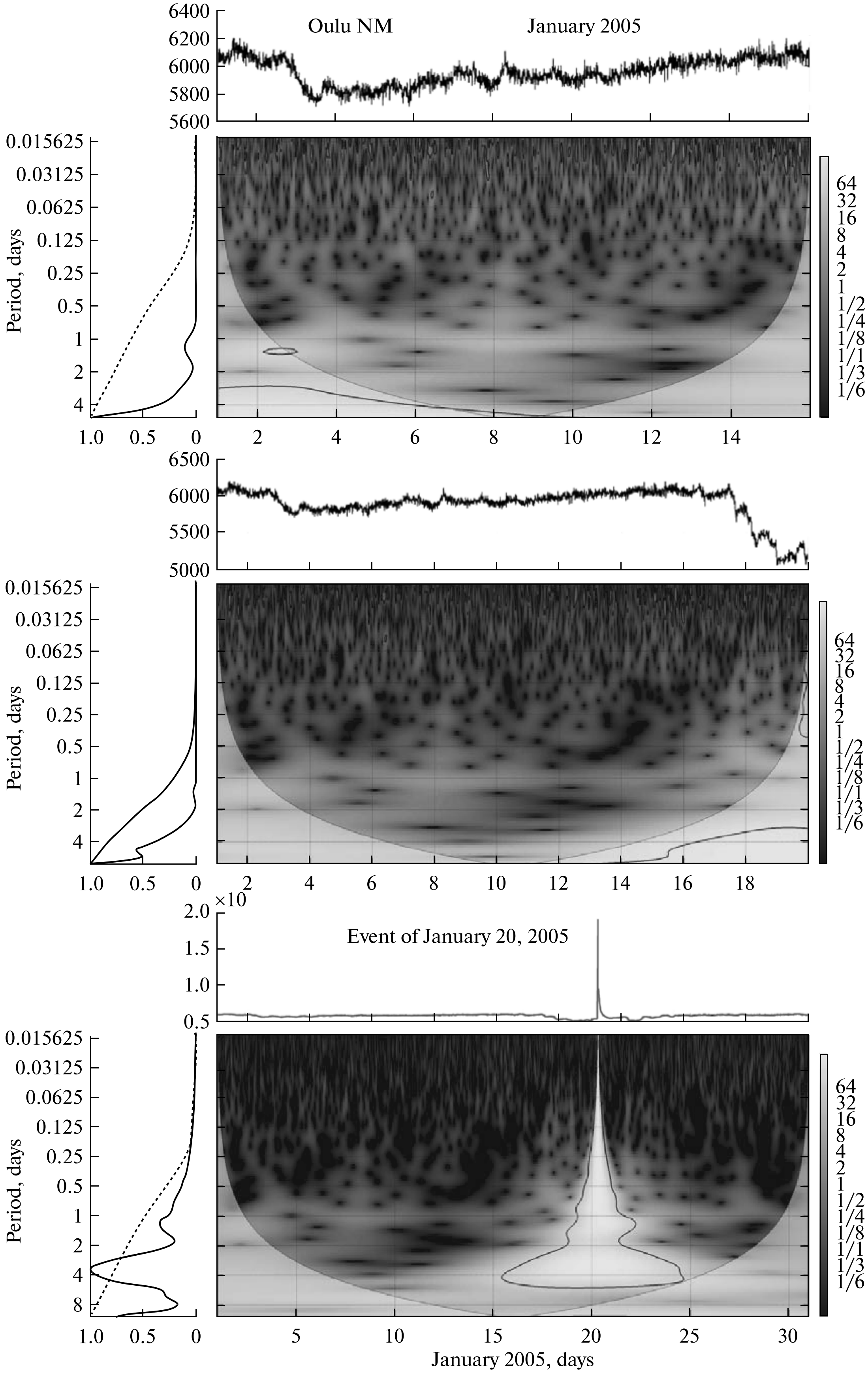
Oulu NM
January 2005
Period, days
Event of January 20, 2005
×10
January 2005, days

Fig. 5. Intensity time profiles and GCR oscillation wavelet spectra five days before the GLE event of January 20, 2005 (the left-hand side panel, top pair of plots); a day (the middle pair) before the GLE event; and on the event day (the bottom pair) with regard to the powerful SCR flux arrival. Intensity plots and wavelet diagrams according to the Oulu data (in NM count rate units) were constructed with different time resolutions; the abscissa axis shows the real time (days in January 2005). The corresponding oscillation power spectra in arbitrary units (the abscissa axis) are shown from top to bottom on the left-hand side panels depending on the period in days (the ordinate axis).

gram were constructed using the Oulu NM data (in arbitrary units); the abscissa axis shows the real time in hours on January 20, 2005; the oscillation periods (the ordinate axis) are given in hours. The power density spectrum of oscillations in arbitrary units (the abscissa axis) is shown on the right-hand side panel, depending on the period in hours (the ordinate axis). Based on Fig. 6, we can conclude that the oscillation power spectrum on the considered event day has the shape of a rather smooth curve covering periods of ≤1 to ~8 h. In this case, the power density plot is much higher than the curve for the calculated red noise in contrast to the other extreme event—GLE05.

Based on the analysis performed by us for four GLE events, we can see that the GCR oscillation periods (frequencies) evolve in the course of time. The evolution begins from small periods (high frequencies) several days before a GLE event; the period increases (the frequency decreases) as the event day approaches. A similar behavior of periods (frequencies) is not observed during the control periods, i.e., outside the intervals where GLE events are registered at least for the four extreme events studied by us. In this case, the characteristic periods of oscillations are formed with different lead times for each event. For example, this took place with an anticipation period from 14 days to one day in the GLE05 case and from 4 days to several hours for the GLE69 event. On the event days, all oscillation periods (frequencies) are present simultaneously, forming specific “wings” (quasi-continuum) in the region of short periods (high frequencies). As was mentioned above, the appearance of high frequencies can be caused by the predominant contribution of SCR flux oscillations. A wavelet analysis of each of the four GLE events indicates that oscillations with different periods are present on the event day in all four cases and most oscillations are generally in the range from ~15 min to ~10 h. However, the results of the conducted GCR oscillation analysis before the studied four GLE events are generally limited. To reliably elucidate how much the GCR oscillation spectrum changes just before the SCR arrival, we should analyze a larger number of cases. A more detailed analysis of control periods (in the absence of a GLE) should also be performed in this case.

4. RATE OF GLEs REGISTRATION

In contrast to GCR oscillations that mainly give diagnostic information about the conditions of the accelerated solar particle transport in the interplanetary medium before a GLE, the registration rate of such events (η) is an absolutely different aspect in SCR physics. As was mentioned above (see Section 3), the fact of individual GLE registrations can be affected by observation conditions. However, the 70-year experience in studying SCRs indicates that parameter η mainly depends on variations in the time properties of their generator (the Sun). Therefore, we will discuss the problem of GLE occurrence rate in more detail.

As is known, the first GLEs (before 1956) were registered at a small number of stations, which were mainly equipped with devices for measuring one hard (mu-meson, or muon) component, i.e., counter muon telescopes (MTs) and ionization chambers (ICs). These standard detectors at sea level have effective energies of ~15–20 and 25–35 GeV, respectively; at the same time, the effective registration energy for neutron monitors is ~4–6 GeV (Miroshnichenko, 2001). From this, it follows that neutron monitors are more sensitive to GLE registration than MTs and ICs. A special technique (e.g., Shea and Smart, 1982; Vashenyuk et al., 2006), which takes into consideration the anisotropy of the SCR flux arrival to the Earth, steep energy spectrum of this radiation, and the high sensitivity of neutron monitors, is used to identify GLEs based on data from the global NM network. At the same time, it is known that certain weak GLEs (from ≥1 to 10%) were mainly registered at high-latitude NMs or at polar stations only (see, e.g., (Kepicova et al., 1982; Shea and Smart, 1987)).

Thus, we can confidently assume that certain weak GLEs were not registered in the first years of SCR observations (before the creation of the global cosmic ray network of stations). In this case, the GLE registration rate was most probably decreased, since some events were a fortiori omitted for technical and methodical reasons. Judging by the average GLE occurrence rate ($\eta \sim 1.0$ event per year), the number of events omitted in 1942–1956 could be considerable: indeed, only four of 14 anticipated “statistically average” events have been registered before 1956 (Miroshnichenko and Pérez-Peraza, 2008). The total time series (70 GLES) was eventually depleted by weak events. On the other hand, GLEs were not observed after GLE70 (December 13, 2006; cycle 23) and up to GLE71 (17 May 2012, current cycle 24), i.e., during more than 5 years, there was observed no one similar event. A similar feature in the GLE registration rate was also observed in the two previous SA cycles. Thus, more than five and almost five years passed between GLE39 (February 16, 1984) and GLE40 (July 25, 1989) and between GLE54 (November 2, 1992) and GLE55 (November 6, 1997), respectively. Note that

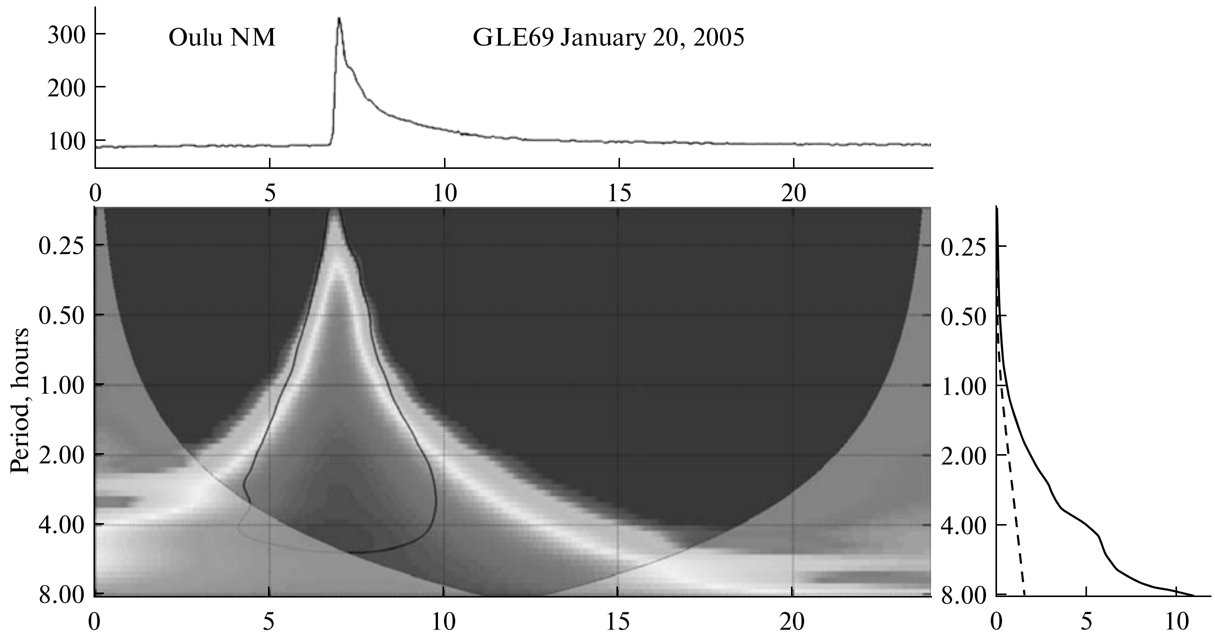

Fig. 6. Intensity time profile and wavelet spectrum of CR flux oscillations on the event day of January 20, 2005 (the left-hand side panel). An intensity plot and wavelet diagram were constructed using the Oulu data (in arbitrary units); the abscissa axis shows the real time in hours on January 20, 2005; the oscillation periods (the ordinate axis) are given in hours. The corresponding oscillation power density spectrum in arbitrary units (the abscissa axis) is shown on the right-hand side panel depending on the period in hours (the ordinate axis).

cycle 24 is developing in a very flabby manner, and the sunspot formation and the flare and "proton" activity of the Sun are generally on a rather low level in spite of the fact that the strongly prolonged cycle 23 minimum ended in December 2009. Despite the considered limitation of the model (analog) PWM series, certain regularities are nevertheless observed in this series (Fig. 7).

An analog PWM series of the GLE rate, constructed based on event registration dates using the Morlet method (Pérez-Peraza et al., 2009), is shown at the top of Fig. 7; a wavelet diagram of the event rate fluctuation is presented at the bottom; and the oscillation power density spectrum for (η) is demonstrated on the right-hand side. We can formally state that oscillations η with periods of ~2.5, 5–8, 11, 22–30, and 60 days are observed in the power spectrum in addition to the well-known SA periodicities with medium and long periods (0.3, 0.5, 0.7, 1.3, 3.5, 7.0, and 11 years). However, most of these periods factually bear a low power level or are near or even lower than the curve for the red noise power, so that only periods of ~0.7, ~7.0, and ~11 years can be considered statistically significant. It is clear that the final judgments concerning the significance of certain peaks in the power spectrum can strongly depend on the general GLE statistics and on the selected red noise model (Torrence and Compo, 1998).

In Figs. 8 and 9, we illustrate a wavelet analysis of the coherence between the analog PWM series for η during the entire observation period (1942–2006) and usual (digital) time series for the SS and CI daily values, respectively. Figure 8 (top right-hand side panel) indicates that the GLE number, in particular, does not follow the SA cycle amplitude (height) with respect to the SS number: e.g., the relatively weak cycle 23 had a larger number of SCR events than the much stronger cycle 22. Approximately the same coherence pattern was found between the GLE occurrence rate and the CI (Fig. 9, top right-hand side panel). Proceeding from an analysis of both coherence spectra (Figs. 8, 9; left-hand side panels), we should acknowledge that the periodicity related to the 11-year solar cycle is controlling (predominant) in both cases and the remaining periodicities are in a region substantially lower than the reliability curve for the red noise power. As one would expect, the SCR event registration rate is higher near the solar cycle maximum. On the other hand, the GLE occurrence rate is apparently independent of the solar cycle amplitude (height) with respect to the SS number.

5. DISCUSSION AND CONCLUSIONS

Recently, Kilcik et al. (2010) studied the periodicities in the solar flare index (SFI) behavior. They analyzed the data obtained for the last three SA cycles: from June 1, 1976, to August 31, 1986 (cycle 21); from September 1, 1986, to March 31, 1996 (cycle 22); and from April 1, 1996, to December 31, 2007 (cycle 23). These researchers used two new methods: (1) the multitaper method (MTM) (Percival and Walden, 1993),

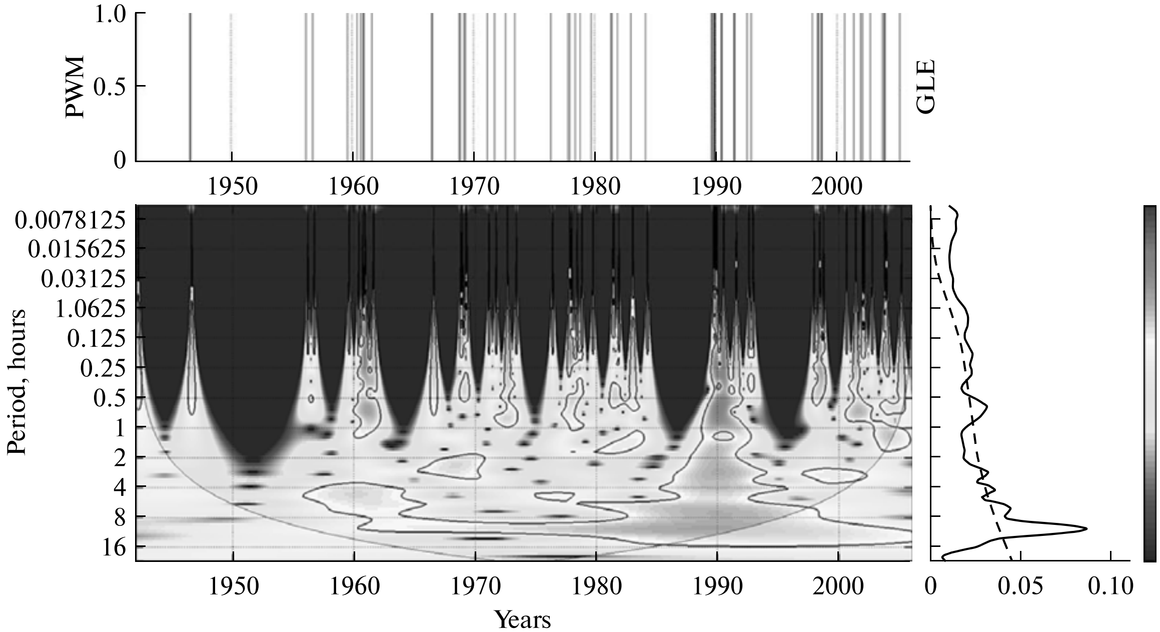

Fig. 7. Occurrence rate oscillations for GLE events. The PWM time series for the GLE occurrence rate (constructed using the Morlet method (Pérez-Peraza et al., 2009) by the registration dates of 70 events in 1942–2006) is given on the top panel; a wavelet diagram for the oscillation spectrum is shown on the bottom panel (the periods in year fractions are presented along the ordinate axis). The oscillation power density spectrum in arbitrary units (the abscissa axis) is shown on the right-hand side depending on the period as a fraction of the year (the ordinate axis).

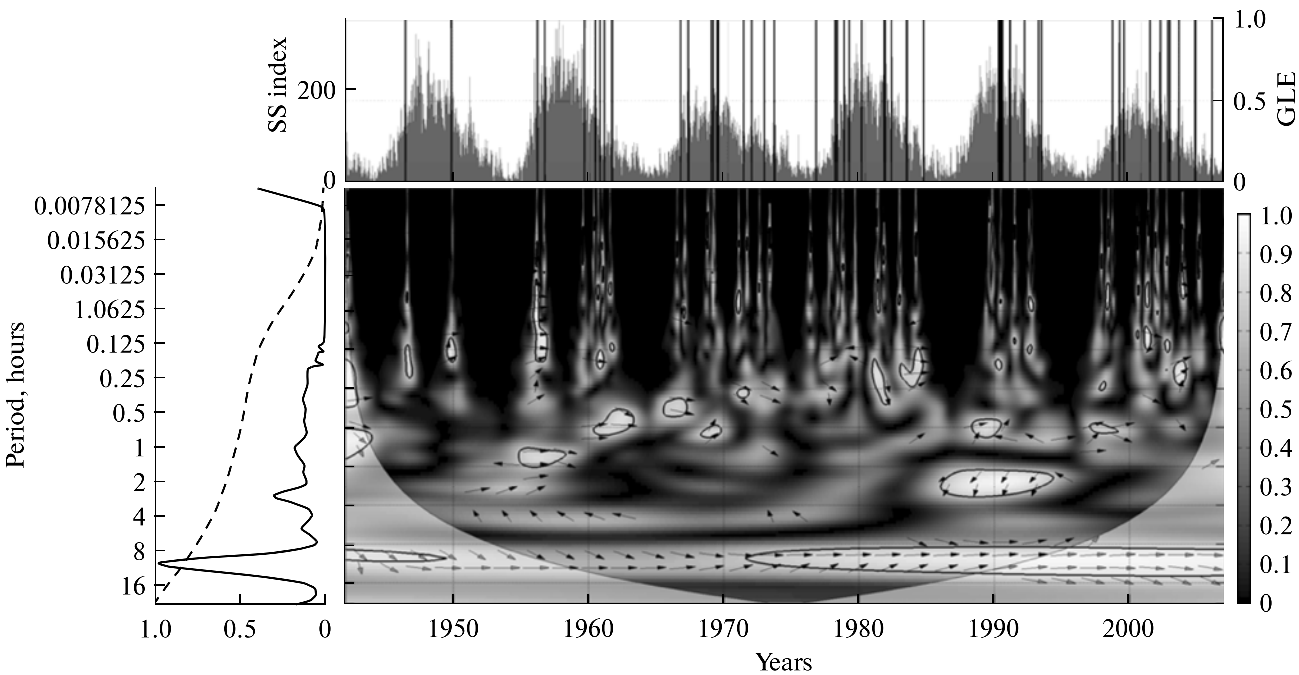

Fig. 8. Coherence evolution between the PWM series for the GLE registration rate (thin vertical lines on the top plot, the right-hand-side scale) and the SS number (gray filling, the left-hand side scale). The entire observation interval (years) is shown on the abscissa axis. The oscillation power density spectrum in arbitrary units (the abscissa axis) is presented on the left-hand side panel depending on the oscillation period as a fraction of the year (the ordinate axis).

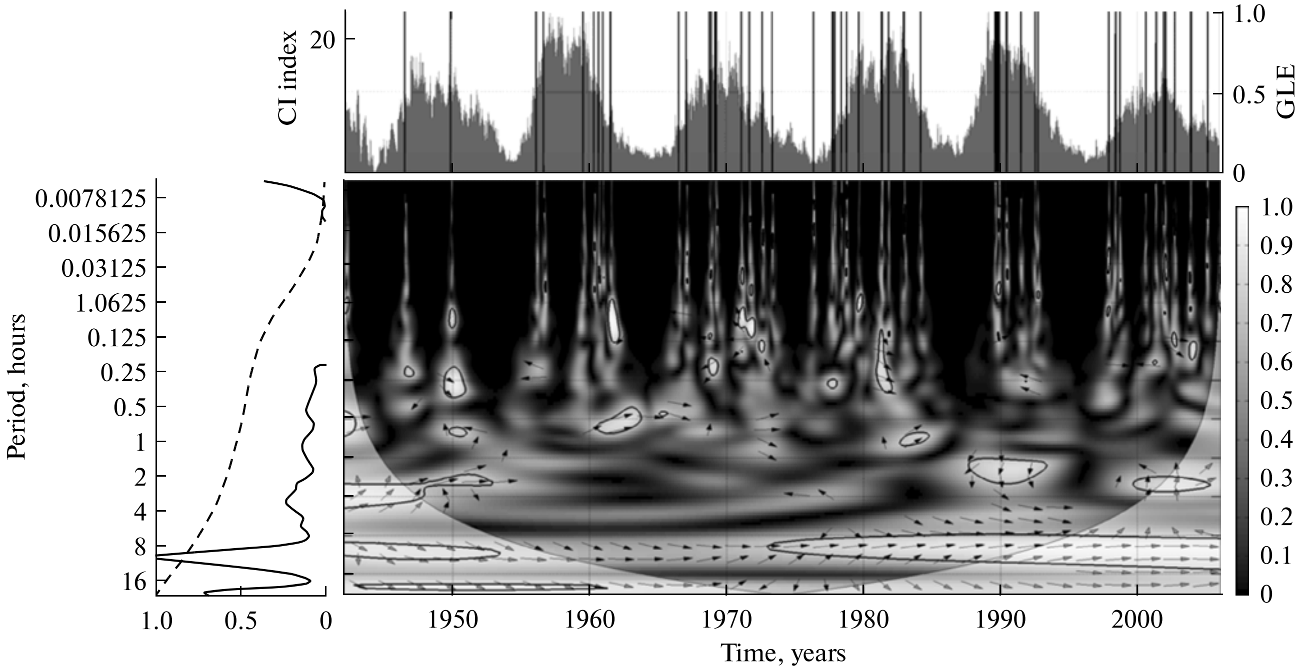

Fig. 9. Coherence evolution between the PWM series for the GLE registration rate (thin vertical lines on the top plot, the right-hand side scale) and the CI value (gray filling, the left-hand side scale). The entire observation interval (years) is shown on the abscissa axis. The oscillation power density spectrum in arbitrary units (the abscissa axis) is presented on the left-hand side panel depending on the oscillation period as a fraction of the year (the ordinate axis).

i.e., the multiconic method with two approximations (for the cases of red and white noise) and (2) the Morlet wavelet transform. In all studied solar cycles at a significance level of at least 90%, they found a period of ~27 days, which is of an evident origin (the solar rotation period). In addition, these authors obtained the following distinct periods: 152, 73, and 62 days for cycles 21, 22, and 23, respectively. However, in this case, they noted that the statistical significance of the obtained periods depended on the applied analysis methods.

In the present work, we for the first time tried to obtain the GCR oscillation spectra before the arrival of relativistic solar protons to the Earth (GLE-type events), using rigorous wavelet analysis methods, and to estimate the coherence (relationship) between certain SA characteristics and the SCR generation rate (η) on the Sun. We analyzed data on the GCR and SCR intensity variations during 1942–2006 and daily values of the SS number and CI for solar cycles 17–23.

In addition to the GCR intensity oscillations, we studied oscillations in the SS and CI indices and the GLE event rate (η). Using four great SCR events as an example (February 23, 1956; July 14, 2000; October 28, 2003; and January 20, 2005), it was shown that the GCR oscillation period (frequency) gradually increases (decreases) as the GLE day approaches. This can be a certain prognostic criterion. Several short-term oscillations were found in addition to the well-known SA periods (0.3, 0.5, 0.7, 1.3, 3.5, 7, and 11 years) in the parameters of the photosphere (SS) and solar corona (CI) (Pérez-Peraza et al., 2009). Periods of 2.5, 5, 11, 22, and 60 days are the most pronounced ones among the discovered periods and are apparently the harmonics of the 11-year solar cycle. Thus, oscillations in the SS, CI, and GCRs obey the hierarchy principle.

Oscillations in the GLE event rate are apparently of an absolutely different nature. Using wavelet analysis, we confirmed here that the PWM series for parameter η includes a statistically significant oscillation with a period of ~11 years. In this case, it turned out that there is certain coherence between oscillations in the GLE rate and the time series of the solar photosphere indices (parameters), e.g., the SS number, and the corona (e.g., with periodicities in the CI behavior). The wavelet diagrams of coherence indicate that the PWM series of GLE events is in phase with the time series for the SS and CI solar indices during the entire studied period (1942–2006). Although the GLE statistics is limited and there are the restrictions imposed by the wavelet analysis methods, the obtained results can be of interest for understanding periodic phenomena in the solar dynamo, solar atmosphere, interplanetary medium, and CRs.

The tendency of GLE events to group mainly on the ascending and descending branches of solar cycles is apparently caused by the specific features of the spatio-temporal structure of the global solar magnetic field (GSMF). As is known, this field's reconfiguration (sign reversal) takes place precisely near SA maximums. Therefore, it is reasonable to consider the interesting results obtained in (Nagashima et al., 1991). These authors used muon telescope and neutron monitor data for 43 GLEs in 1942–1990 (the end of cycle 17–the middle of cycle 22) in order to analyze the above GLE tendency. They indicated that flares that cause GLEs are essentially forbidden during the cycle transitional stage, when the GSMF changes its sign. Nagashima et al. (1991) explain the absence of GLEs at SA maxima (at least for cycles 17–21) by a deterioration of the efficiency of particle acceleration during the GSMF re-arrangement in the transition period rather than by the suppression of SCR production and release because of strong magnetic fields. Already in cycle 22, the GLE occurrence rate increased sharply and the event number was anomalously large (15). In this case, seven events took place during five months when an SS maximum was reached (July 1989), and the remaining eight events were observed when the GSMF changed its sign (1991–1992). It is absolutely evident that certain conclusions require additional studies. In particular, it is necessary to study the structure and dynamics of large-scale magnetic fields in the solar corona for individual events, such as the event that occurred on September 29, 1989 (GLE42), in order to separate the SCR acceleration effects and release from the solar atmosphere (Miroshnichenko et al., 2000).

Since some periodicities found in the present work are coherent for the η, SS, and CI parameters, at this stage of studies, we can conclude that oscillations are synchronized in the solar atmosphere from the photosphere to the corona. This can indicate that the SCR generation affects considerable regions in the solar atmosphere and it is not a local (isolated) process typical of only chromospheric or coronal structures.

A more disputable result of our work consists in that we can find a common criterion for predicting SCR events based on the specific GCR oscillation behavior several weeks (days) before a GLE event by the observations at one or several NM stations. In any case, we can render software in order to perform a wavelet analysis according to the Morlet scheme at one or several stations (e.g., Oulu (Firoz et al., 2010)) where GCR oscillations can be controlled every day. Thus, we could verify whether the proposed method could be theoretically and effectively used to predict GLEs with a lead time of several days. Tentative prognosis (Pérez-Peraza et al., 2011) indicated that the next GLE71 may be expected between 12 December 2011 and 2 February 2012. Effectively, it happened on 17 May 2012. The event turned out to be rather small (about 14–16% by 5-minute data of NMs) and was detected at high latitudes only.

It is reasonable to note that a similar wavelet analysis for the SS number and GCR flux (Christiansen et al., 2007) demonstrated a considerable and even strong anticorrelation between their oscillations during the entire observation period but for periods of ≥7 years only; however, a distinct correlation (anticorrelation) between signals is absent when periods are shorter. Thus, the SS can only be a good indicator of GCR variations on large time scales. The GCR oscillation distribution can be used to study a solar cycle, predict solar proton events, and in other practical applications in the space weather problem.

Thus, the up-to-date wavelet analysis methods allowed us to demonstrate visually the GCR flux oscillation pattern before and during SCR events and indicate that SS and CI oscillations are closely related to (coherent with) the GLE occurrence rate. At that, we obtained the first indications that SCR generation processes can be synchronized with periodic processes in the solar dynamo, solar atmosphere, interplanetary medium, and GCRs. At the same time, similar studies of solar and geophysical phenomena indicated that researchers should very carefully apply the wavelet analysis technique and take into account all possible factors that can affect the wavelet transform of the initial data series. As an example, we mention the results obtained by De Moortel et al. (2004), who demonstrated that the application of two different mother wavelets to an analysis of two observed solar oscillation types (using the TRACE spacecraft data) leads to strongly different results.

ACKNOWLEDGMENTS

We are highly grateful to the reviewer for a number of constructive critical remarks, which made it possible to substantially improve the paper. We thank all researchers whose data were used in the present work, as well as the authors of the corresponding software for wavelet analysis (Torrence and Compo, 1998), located on the site http://paos.colorado.edu/research/wavelets.

This work was supported by the Universidad Nacional Autonoma de Mexico (Mexico), DGAPA grants PAPIIT: IN1170009, DGAPA: INI 19209-3, IXTLI: 0709013, and CONACYT of Mexico: 089887. The work was partially supported by the Russian Foundation for Basic Research (projects nos. 07-02-01405, 08-02-92208, 09-02-98511, and 11-02-08034). The work was supported by a target Federal scientific and technical program; by the Russian Academy of Sciences (Basic Research Program no. 16 (OFN-16)); and by the grants of President president of the Russian Federation (nos. NSh-8499.2006.2 and NSh-4573.2008.2).

REFERENCES

Christiansen, F., Haigh, J.D., and Lundstedt, H., Influence of Solar Activity Cycles on Earth's Climate, in *Exclusive Summary Report, ESTED Contract no. 18453/04/NL/AR*, issue 1, 2007.

Chui, K., *Vvedenie v veilety* (Introduction to Wavelets), Moscow: Mir, 2001.

De Moortel, I., Munday, S.S., and Hood, A.W., Wavelet Analysis: The effect of Varying Basic Wavelet Parameters, *Sol. Phys.*, 2004, vol. 222, no. 2, pp. 203–228.

Firoz, K.A., Cho, K.-S., Hwang, J., et al., Characteristics of Ground-Level Enhancement-Associated Solar Flares, Coronal Mass Ejections, and Solar Energetic Particles, *J. Geophys. Res.*, 2010, vol. 115, p. A09105; doi:10.1029/2009JA015023.

Gilman, D. L., Fuglister, F. J., and Mitchell, J. M., Jr., On the Power Spectrum of "Red Noise", *J. Atmos. Sci.*, 1963, vol. 20, no. 2, pp. 182–184.

Grinsted, A., Moore, J., and Jevrejera, S., Application of the Cross Wavelet Transform and Wavelet Coherence to Geophysical Time Series, *Nonlinear Proc. Geophys.*, 2004, vol. 11, no. 5/6, pp. 561–566.

Holmes, D.G. and Lipo, T.A., *Pulse Width Modulation for Power Converters: Principles and Practice*, Wiley, 2003.

Kepicova, O., Miroshnichenko, L.I., and Stehlik, M., Analysis of Solar Cosmic Ray Increases of September 1977 Based on Ground-Level Data, *Phys. Solariterrestris*, 1982, no. 19, pp. 40–52.

Kilcik, A., Ozguc, A., Rozelot, J.P., and Atac, T., Periodicities in Solar Flare Index for Cycles 21–23 Revisited, *Sol. Phys.*, 2010, vol. 264, pp. 255–268; doi: 10.1007/s11207-010-9567-7.

Koronovskii, A.A. and Khramov, A.E., *Nepreryvnyi veivletnyi analiz i ego prilozheniya* (Continuous Wavelet Analysis and Its Applications), Moscow: Fizmatlit, 2003.

Kumar, P. and Foufoula-Georgiou, E., Wavelet Analysis for Geophysical Applications, *Rev. Geophys.*, 1997, vol. 34, pp. 385–412.

Mendoza, B., Velasco, V.M., Valdes-Galicia, J.F. Mid-term Periodicities in the Solar Magnetic Flux. *Solar Phys.*, 2006, V. 233. no. 2. pp. 319–330.

Miroshnichenko, L.I., Cyclic Variations and Sporadic Fluctuations of Solar Cosmic Rays, *Biofizika*, 1992, vol. 37, no. 3, pp. 364–377.

Miroshnichenko, L.I., *Solar Cosmic Rays*, Dordrecht: Kluwer, 2001.

Miroshnichenko, L.I., *Radiation Hazard in Space*, Dordrecht: Kluwer, 2003.

Miroshnichenko, L.I., Radiation Field Formation and Monitoring beyond LEO, *Adv. Space Res.*, 2005, vol. 36, no. 9, pp. 1742–1748.

Miroshnichenko L.I. and Pérez-Peraza, J., Astrophysical Aspects in the Studies of Solar Cosmic Rays, *Int. J. Mod. Phys. A*, 2008, vol. 23, no. 1, pp. 1–141.

Miroshnichenko, L.I., de Koning, C.A., and Pérez-Enríquez, R., Large Solar Event of September 29, 1989: Ten Years after (Review), *Space Sci. Rev.*, 2000, vol. 91, pp. 615–715.

Nagashima, K., Sakakibara, S., and Morishita, I., Quiescence of GLE-Producible Solar Proton Eruptions during the Transition Phase of Heliomagnetic Polarity Reversal near the Solar Activity-Maximum Period, *J. Geomagn. Geoelectr.*, 1991, vol. 43, no. 8, pp. 685–689.

Percival, D.B., and Walden, A.T., *Spectral Analysis for Physical Applications — Multitaper and Conventional Univariate Techniques*, Cambridge: Cambridge Univ. Press, 1993.

Percival, D.B. and Walden, A.T., *Wavelet Methods for Time Series Analysis*, Cambridge: Cambridge Univ. Press, 2000.

Pérez-Peraza, J., Velasco, V.M., Zapotitla, J., Vashenyuk, E.V., and Miroshnichenko, L.I., Pulse Width Modulation Analysis of Ground Level Proton Events, *Proc. 31st Int. Cosmic Ray Conference*, Lodz, 2009.

Pérez-Peraza, J., Velasco-Herrera, V.M., Zapotitla, J., Miroshnichenko, L.I., and Vashenyuk, E.V., Search for Periodicities in Galactic Cosmic Rays, Sunspots, and Coronal Index before the Arrival of Relativistic Protons from the Sun, *Izv. Ross. Akad. Nauk, Ser. Fiz.*, 2011a, vol. 75, no. 6, pp. 816–818.

Pérez-Peraza J., Velasco-Herrera V., Zapotitla J., Miroshnichenko L.I., Vashenyuk E.V., and Libin I.Ya. Classification of GLEs as a Function of their Spectral Content for Prognostic Goals, Proc. 32nd Int. Cosmic Ray Conf., Beijing, China, 11–18 August 2011. V. 10. pp. 149–152. 2011b.

Reames, D.V., Particle Acceleration at the Sun and in the Heliosphere, *Space Sci. Rev.*, 1999, vol. 90, pp. 413–491.

Shea, M.A., and Smart, D.F., Possible Evidence for a Rigidity-Dependent Release of Relativistic Protons from the Solar Corona, *Space Sci. Rev.*, 1982, vol. 32, no. 1/2, pp. 251–271.

Shea, M.A., and Smart, D.F., Relativistic Solar Proton Events during the SMY–SMA, in *Solar Maximum Analysis*, Stepanov, V.E. and Obridko, V.N., Eds., Utrecht: VNU Sci. Press, 1987, pp. 309–314.

Torrence, C. and Compo, G.P., A Practical Guide to Wavelet Analysis, *Bull. Am. Meteorol. Soc.*, 1998, vol. 79, pp. 61–78; doi: 10.1175/1520-0477.

Vashenyuk, E.V., Regularities in the Manifestation of Events with Relativistic SCRs, *Astron. Vestn.*, 2000, vol. 34, no. 2, pp. 173–176.

Vashenyuk, E.V., Balabin, Yu.V., Pérez-Peraza, J., Gallegos-Cruz, A., and Miroshnichenko, L.I., Some Features of the Sources of Relativistic Particles at the Sun in the Solar Cycles 21–23, *Adv. Space Res.*, 2006, vol. 38, no. 3, pp. 411–417.

Velasco, V.M., and Mendoza, B., Assessing the Relationship between Solar Activity and Some Large Scale Climatic Phenomena, *Adv. Space Res.*, 2008, vol. 42, pp. 866–878.

Velasco, V.M., Mendoza, B., and Valdes-Galicia, J.F., The 120-Yrs Solar Cycle of the Cosmogenic Isotopes, *Proc. 30th Int. Cosmic Ray Conference*, Caballero, R., D'Olivo, J.C., Medina-Tanco, G., Nellen, L., Sánchez, F.A., and Valdés-Galicia, J.F., Eds., Mexico, 2007, vol. 1, pp. 553–556.